

# Excimer laser treatment of copper-coated mild steel

C. N. PANAGOPOULOS, A. MARKAKI

*Laboratory of Physical Metallurgy, National Technical University of Athens, Zografos, 15780, Athens, Greece*

E. HONTZOPOULOS

*Institute of Electronic Structure and Laser, University of Crete, Iraklion, Greece*

Copper-coated mild steel specimens were irradiated with a high power excimer laser. Mild steel was first coated with a thin nickel coating. Laser-induced surface structures were observed by means of optical microscopy. The surface roughness was observed to be dependent on the number of pulses per step. Energy dispersive X-ray (EDX) analysis showed that nickel and iron atoms diffused into the copper coating. The microhardness of the copper coating was found to increase after laser treatment due to solid solution strengthening from iron and nickel atoms.

## 1. Introduction

The use of laser beam technology to improve the properties of the near surface region, which can determine the performance of a material, has been extensively studied. Laser surface alloying is a fast and efficient technique for producing surface layers with improved properties. The alloying elements can be added by pre- or codeposition methods.

Surface treatments by means of laser beam radiation are performed today on an industrial and research scale mainly by using a continuous CO<sub>2</sub> laser. The most important problem of this laser arises from the high reflectivity of light at 10.6 μm. This problem can be overcome by using Nd–YAG or excimer lasers [radiation in the visible and ultraviolet (u.v.) wavelength ranges, respectively] that have shorter wavelengths and the capabilities of giving very high pulse energies, reducing the problems due to the reflection. However, it should be noted that in comparison with continuous lasers, CO<sub>2</sub>, pulsed Nd–YAG and excimer lasers are not as flexible and emit lower power levels [1].

Some of the recent studies in the technological field of surface alloying with a pulsed laser are listed below:

Wang and Spaepen [2] studied the formation of Nb–Si alloys by pulsed laser radiation, using an Nd–YAG laser, or multilayered films of Nb and Si on a copper substrate. The lattice parameters of these solid solutions suggest that the solute atoms can be interstitial or substitutional.

Lin and Spaepen [3] using pulsed laser treatment with Nd–YAG created Ni–Nb alloys of multilayered films of Ni and Nb on a copper substrate, which was first coated by an evaporated Al film. This work presented the effects of quenching on the extension of primary solubility and the occurrence of intermetallic compounds.

Hirvonen *et al.* [4] have implanted Ti ions into Fe surfaces forming a thin amorphous surface alloy by excimer laser irradiation. This alloy improves the wear and friction properties of the surface as compared with the unimplanted surface.

Jervis *et al.* [5] studied the formation of amorphous Ti alloy layers by excimer laser mixing of Ti on AISI 304 stainless steel surfaces. The laser mixing process, unlike Ti ion implantation, does not result in high incorporation of C in the processed layer.

Michaelides and Panagopoulos [6] examined electrodeposited zinc on a copper substrate irradiated with an excimer laser. Zinc atoms were found to diffuse into the copper substrate. The surface morphology and structure after laser treatment were examined.

Panagopoulos *et al.* [7] irradiated electroplated zinc on an aluminium substrate with a high power excimer laser. Zinc atoms were found to diffuse into the substrate. The microstructure of the surface after laser treatment was mainly dendritic. The surface roughness was a function of the lasing conditions.

Das [8] studied pure aluminium after surface laser alloying with nickel using an Nd–YAG laser pulse. It was observed that the surface roughness of the alloyed surface decreased with an increase in the extent of defocusing of the laser beam.

By using a Nd–YAG laser, Tayal and Mukherjee [9] achieved laser boriding of low carbon steel. High hardness values were obtained due to the variety of microstructure.

The work described in this paper aimed to produce surface alloys on copper-coated mild steel after interaction with very short pulses of a high intensity excimer laser beam. The copper coating was electrodeposited on mild steel prior to laser treatment. An evaluation of the effect of the lasing conditions on the

surface of copper-coated mild steel is made, together with a determination of the elemental concentration in the alloyed surfaces and hardness measurements.

## 2. Experimental procedure

The substrate material was mild steel with a carbon content of 0.07 wt %. Specimens with dimensions of  $3.0 \times 1.0 \text{ cm}^2$  and thicknesses of 0.5 mm were used in this study.

The specimens were annealed at  $550^\circ\text{C}$  for about 2 h, to eliminate residual stresses resulting from machining. The methods used to prepare the surface of the substrate for electrodeposition was alkaline cleaning (in a solution of 0.2 M NaOH at  $70^\circ\text{C}$  for 20 min) and acid pickling with an inhibitor (HCl acid for a few minutes). Afterwards the specimens were mechanically polished with a series of SiC papers (Nos 220, 400, 600 and 800).

Copper electrodeposition took place in an acid sulphate bath. The composition of the bath and the operating condition were:  $220 \text{ g l}^{-1} \text{ CuSO}_4$  and  $60 \text{ g l}^{-1} \text{ H}_2\text{SO}_4$  at a temperature,  $T$  of  $35^\circ\text{C}$ .

The current density was kept constant at  $4 \text{ A dm}^{-2}$ . Two thicknesses of copper coating were chosen, i.e. 10 and  $30 \mu\text{m}$ .

When copper is to be deposited in an acid sulphate bath, steel must receive a nickel strike. This prevents deposition of copper by immersion and precludes peeling of the plate [10]. Electrodeposition of nickel took place in a Watts-type bath. The composition of the bath and the operating condition were:  $317 \text{ g l}^{-1} \text{ NiSO}_4 \cdot 6\text{H}_2\text{O}$ ,  $45 \text{ g l}^{-1} \text{ NiCl}_2 \cdot 6\text{H}_2\text{O}$  and  $37 \text{ g l}^{-1} \text{ H}_3\text{BO}_3$  at  $\text{pH} = 3\text{--}3.5$  and  $T = 57\text{--}60^\circ\text{C}$ .

The current density was kept constant at  $5 \text{ A dm}^{-2}$ . The thickness of the nickel strike was approximately  $2 \mu\text{m}$ .

The copper-coated mild steel specimens were laser irradiated with a Lambda Physik excimer laser using a KrF gas mixture with wavelength,  $\lambda$ , of  $\lambda = 248 \text{ nm}$ . The laser pulse had a rise time,  $\tau_0$  of 10 ns and a total duration,  $\tau_p$ , of 29 ns. The beam had a Lorentzian intensity profile. Processing was done in air with no shield gas. The area of the incident laser beam was  $1.0 \times 1.0 \text{ cm}^2$ . Each specimen was irradiated under different conditions. The variables of the irradiation were: the power density and the number of pulses per step (p.p.s.). In order to observe the influence of each laser parameter, all the experiments were carried out so that one parameter was kept constant while the other varied. The power density was varied between 150 and  $430 \text{ MW cm}^{-2}$  and the pulses per step was varied between 10 and 250 p.p.s. The overlap between successive steps was 30%, the pulse frequency was 10 Hz and the surface was given a single scan.

After the laser treatment, surface morphology and cross-sections of the copper-coated mild steel specimens were examined by means of a Zeiss optical microscope.

Cross-sections embedded in epoxy were used to determine the depthwise variation in elemental concentration with an EDX spectrometer of a scanning electron microscope (Jeol-6300).

The laser-treated specimens were examined with a Philips diffractometer with  $\text{CoK}_\alpha$  radiation ( $\lambda = 0.1791 \text{ nm}$ ) and an iron filter.

A Mahr Perthen profilometer was used to measure the roughness of the laser-treated surfaces by moving the stylus parallel to the laser steps. The parameter estimated for this purpose was the deviation of arithmetic mean of the roughness profile,  $R_a$ . For any particular surface,  $R_a$  was measured across ten different profiles and the mean was taken to be the representative value. The error bars in the corresponding figure indicate the standard deviation of each set of results.

Microhardness measurements were made on cross-sections of laser- and non-laser-treated samples, with a Vickers indenter of a Reichert microhardness test instrument. The load was 8 g and the time of loading for each indentation was 15 s. Each hardness value was the average of seven measurements and the standard deviation of each set of results was not greater than 3%.

## 3. Results and discussion

Fig. 1 shows a cross-sectional view of a copper-coated mild steel specimen. The electrodeposition rate of copper from the acid sulphate bath was found to be a linear function of time. The thickness of the coating was metallographically defined.

The laser power density,  $I_0$  at the surface of the copper is assumed to be the actual power per unit area absorbed,  $A \times I_i$ , where  $A$  is the absorptivity and  $I_i$  is the incident laser power density. The solution of the basic heat-transfer equation for the temperature,  $T(z, t)$ , as a function of depth,  $z$ , into the solid copper and time,  $t$ , is given by the following equation [11]

$$T(z, t) = \frac{2I_0}{k} \left[ \left( \frac{\kappa t}{\pi} \right)^{1/2} \exp(-z^2/4\kappa t) - \frac{z}{2} \operatorname{erfc} \frac{z}{(4\kappa t)^{1/2}} \right] \quad (1)$$

where

$$\operatorname{erfc}(s) = \frac{2}{(\pi)^{1/2}} \int_0^s \exp(-x^2) dx \quad (2)$$

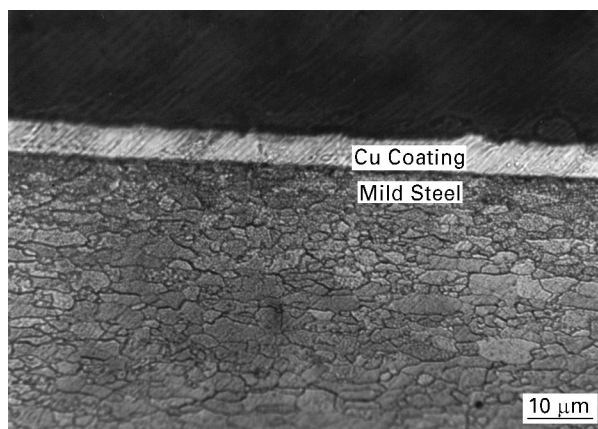


Figure 1 Cross-sectional view of a copper-coated mild steel.

is the error function,  $erfc(s)$  is the complementary error function or  $1 - erf(s)$ .  $\kappa$  is the thermal diffusivity,  $\kappa = k/(\rho \times C)$  (2) where  $k$  is the thermal conductivity,  $\rho$  is the density and  $C$  the specific heat for unit mass.

The surface temperature,  $T_s$ , of copper during its radiation (depth,  $z = 0$ ) is given by the following equation

$$T_s(0, t) = \frac{I_0}{k} \left( \frac{4\kappa t}{\pi} \right)^{1/2} = \frac{A \times I_i}{k} \left( \frac{4\kappa t}{\pi} \right)^{1/2} \quad (3)$$

By using Equation 3 it is possible to estimate the incident power density at the point of impact,  $I_i$ , for a given temperature on the surface,  $T_i$ , and pulse duration,  $\tau_p$  of 29 ns

$$I_i = \frac{k \times T_i}{A} \left( \frac{\pi}{4\kappa\tau_p} \right)^{1/2} \quad (4)$$

The thermophysical constants for copper are:  $k = 3.3 \text{ J s}^{-1} \text{ cm}^{-1} \text{ K}^{-1}$ ,  $\rho = 8.94 \text{ g cm}^{-3}$ ,  $C = 0.385 \text{ J g}^{-1} \text{ K}^{-1}$ .

The absorptivity,  $A$ , at a wavelength,  $\lambda$  of 248 nm has been evaluated a little higher than 60% at room temperature (Fig. 2, absorptivity = 1-reflectivity for opaque materials like copper). The true value in the present case can be expected to be lower. The surface roughness of the specimens before laser treatment was found to be about  $0.40 \mu\text{m}$ . When the surface roughness is greater than the wavelength of the beam ( $0.248 \mu\text{m}$ ), the absorption of radiation decreases due to multiple reflections in the undulations [12].

By replacing the corresponding values in Equation 4, it was found that the threshold value of power density causing copper to melt ( $T_m = 1356 \text{ K}$ ) by using an excimer laser KrF\* source was approximately  $I_m = 43 \text{ MW cm}^{-2}$ . Similarly, the threshold power density required to vaporize copper ( $T_v = 2863 \text{ K}$ ) was approximately  $I_v = 90 \text{ MW cm}^{-2}$ .

In this study, taking into account the previous calculations, the incident power densities ( $150\text{--}430 \text{ MW cm}^{-2}$ ) are enough to cause melting of the surface layer of copper. Because more heat is deposited, the melt front propagates inwards by conduction into the deeper parts of the material until the energy of the

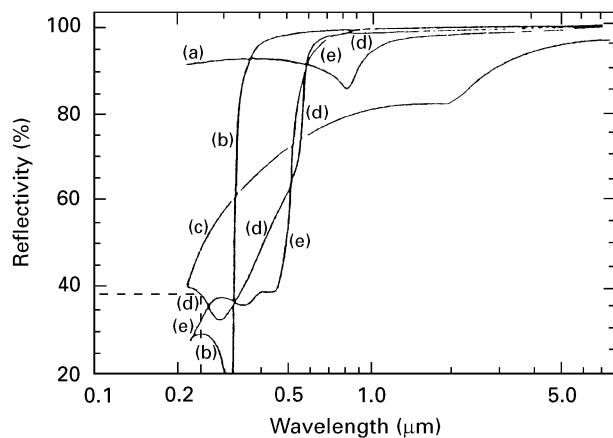


Figure 2 Reflectivity of a number of metals (including copper) as a function of wavelength: (a) Al, (b) Ag, (c) Pt, (d) Cu, and (e) Au.

pulse is totally dissipated. The melt front then stops and a resolidification front moves back towards the free surface.

Micrographs in Figs 3 and 4 show the surfaces of specimens after irradiation by 20 pulses per step at a power density of  $300$  and  $430 \text{ MW cm}^{-2}$ , respectively. Anthony and Cline [13] examined how the surface tension gradients cause rippling (succession of “valleys” and “hills”) of a laser-melted surface. Because the processing takes place during an extremely short period there is no time to flatten and the whole region freezes. Fig. 5 shows a cross-section of a specimen

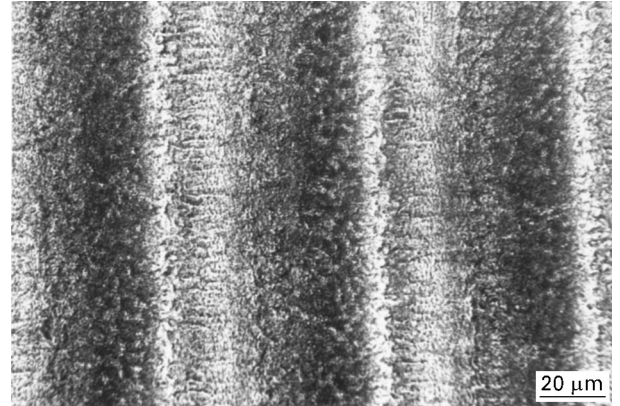


Figure 3 Aspect of the surface of a copper-coated specimen after laser treatment ( $300 \text{ MW cm}^{-2}$  power density, 20 pulses per step).

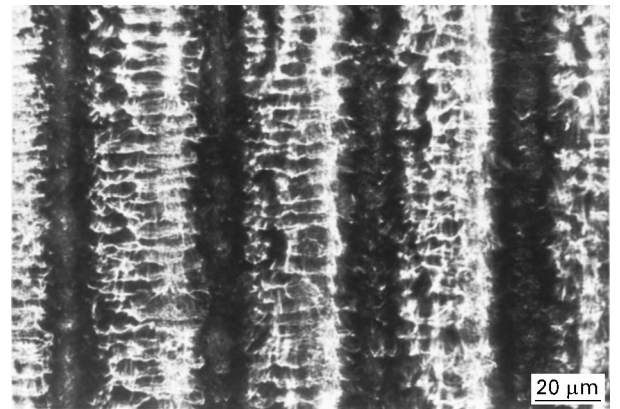


Figure 4 Aspect of the surface of a copper-coated specimen after laser treatment ( $430 \text{ MW cm}^{-2}$  power density, 20 pulses per step).

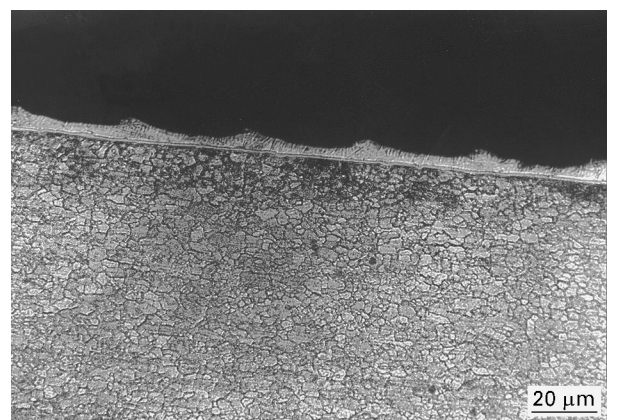


Figure 5 Cross-section of a copper-coated mild steel specimen after laser irradiation ( $430 \text{ MW cm}^{-2}$  power density, 20 pulses per step).

laser irradiated at a laser power density of  $430 \text{ MW cm}^{-2}$ . The presence of “valleys” and “hills” is obvious. The “valleys” (dark areas) correspond to depressed surfaces under the centre of the beam and the “hills” (light areas) to surfaces away from the centre of the beam. Examining Figs 3 and 4 it is observed that the widths of the “hills” (light areas) remain the same and correspond to overlaps between successive steps (30%). The widths of the “valleys” (dark areas) are larger in Fig. 3 than in Fig. 4. The changes in the widths may be attributed to the different values of laser power densities (the number of pulses for both figures is the same). The formation of “valleys” and “hills” is enhanced by the creation of plasma in the copper surface during its excimer laser radiation (previous calculations show that the incident power densities are sufficient to cause evaporation of the surface layer of copper).

Fig. 6 shows the surface roughness,  $R_a$ , of the laser-treated specimens as a function of the number of pulses per step. Increasing the number of pulses leads to increasing absorption of the incident laser energy (as the temperature rises absorption increases because of an increase in the photon population causing more photon–electron energy exchanges [12]) resulting in an increase of the surface roughness.

In the X-ray diffraction data there was evidence for the formation of copper oxide, CuO (Fig. 7). The formation of the oxides may well have been due to strong melt–environment interactions (the experiments were performed in ambient air and the incident power densities were much higher than the threshold value of the power density necessary to melt copper). Also, the plasma creates a charged zone of copper atoms that easily react with oxygen atoms (oxygen molecules decompose due to the high temperature) and form oxides.

During the laser treatment, heat is transferred away from the surface to the internal layers of the copper coating (copper has very high thermal conductivity). Transport of heat during the laser treatment stimulates the mechanism of diffusion in the solid state. The results of microanalysis of some laser-treated specimens are shown in Figs 8 and 9. It was observed that iron atoms from the substrate diffuse into the thin nickel coating and then to the copper coating. Nickel

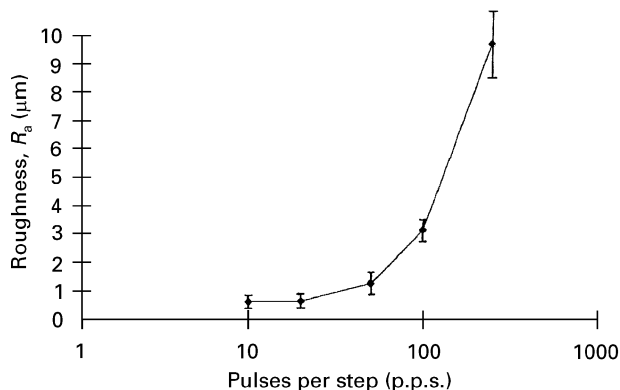


Figure 6 Surface roughness of laser-treated specimens as a function of the number of pulses per step ( $300 \text{ MW cm}^{-2}$  power density).

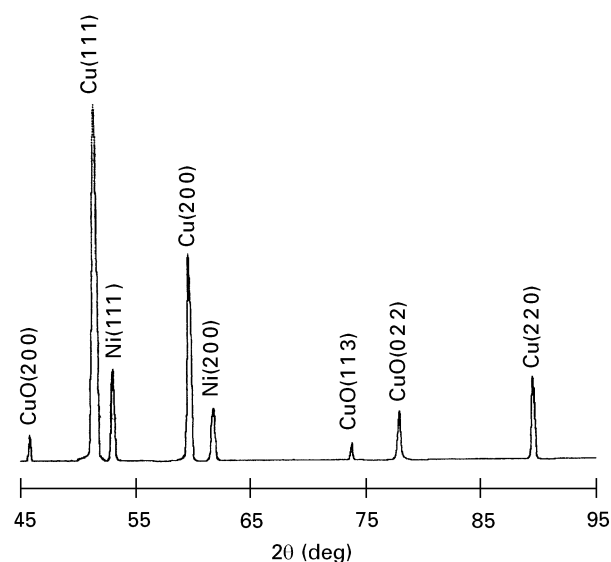


Figure 7 X-ray diffractometry data from the laser-treated surface (the thickness of the copper coating is  $10 \mu\text{m}$ . Lasing conditions:  $300 \text{ MW cm}^{-2}$  power density, 50 pulses per step).

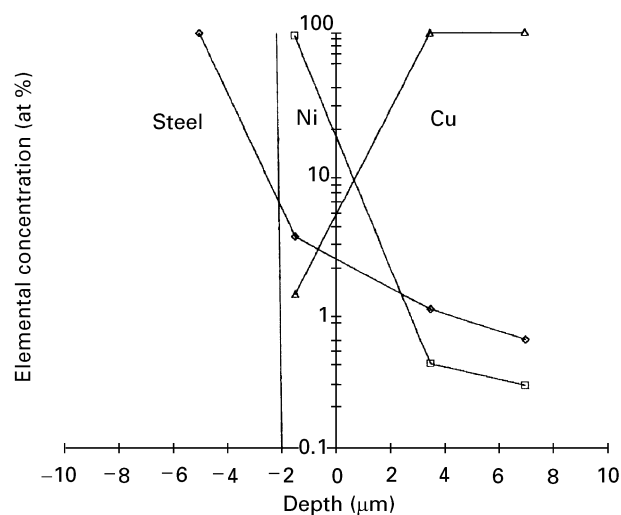


Figure 8 Elemental concentration (at %) as a function of depth (EDX analysis). ( $\diamond$ ) Fe, ( $\square$ ) Ni, ( $\triangle$ ) Cu (thickness of copper coating,  $10 \mu\text{m}$ ; lasing conditions:  $430 \text{ MW cm}^{-2}$  power density at 20 pulses per step).

atoms were found to diffuse into the copper coating. Copper atoms were also found to migrate into the thin nickel coating. Copper and nickel diffusion into the mild steel substrate was not detected.

Examining the results of EDX microanalysis, some observations can be made:

1. As the diffusion distance increases, the number of diffused atoms becomes lower.
2. The concentration profiles of iron are a function of the lasing conditions, in particular, of the power density and the number of pulses per step (Figs 10 and 11, respectively). Increasing each parameter separately, shows that diffusion became weaker.

Figs 12 and 13 show the average microhardness profiles of copper with depth for different lasing conditions.

Comparing the microhardness values before and after the laser treatment, it can be seen that there is

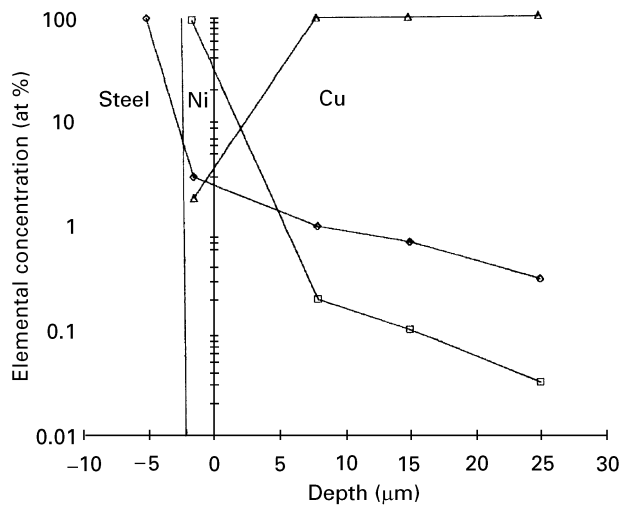


Figure 9 Elemental concentration (at %) as a function of depth (EDX analysis). ( $\diamond$ ) Fe, ( $\square$ ) Ni, ( $\triangle$ ) Cu (thickness of copper coating, 30  $\mu\text{m}$ ; lasing conditions: 300  $\text{MW cm}^{-2}$  power density at 20 pulses per step).

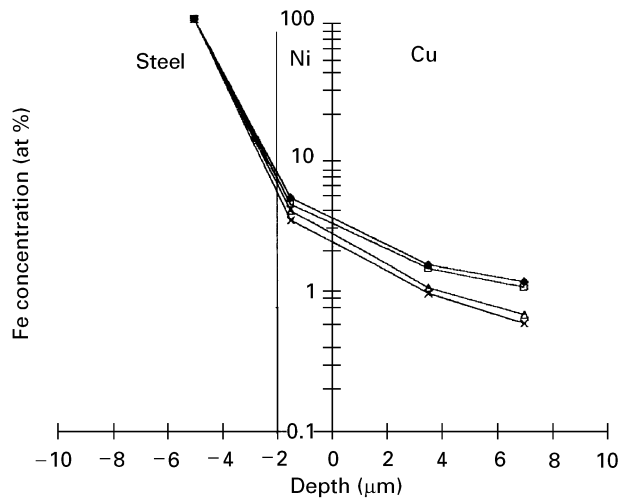


Figure 10 Iron concentration (at %) as a function of depth (EDX analysis): ( $\blacklozenge$ ) 150  $\text{MW cm}^{-2}$ ; ( $\square$ ) 200  $\text{MW cm}^{-2}$ ; ( $\triangle$ ) 350  $\text{MW cm}^{-2}$ ; ( $\times$ ) 430  $\text{MW cm}^{-2}$ . (Thickness of copper coating, 10  $\mu\text{m}$ ; lasing conditions: 20 pulses per step).

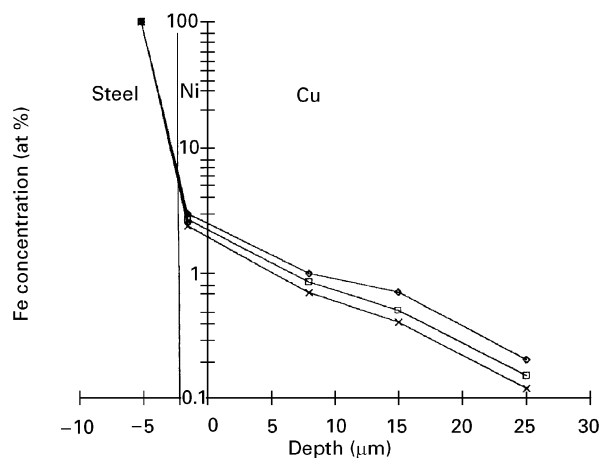


Figure 11 Iron concentration (at %) as a function of depth (EDX analysis): ( $\diamond$ ) 20 p.p.s., ( $\square$ ) 100 p.p.s., ( $\times$ ) 250 p.p.s. (thickness of copper coating, 30  $\mu\text{m}$ ; lasing conditions: 300  $\text{MW cm}^{-2}$ ).

a small increase due to the laser treatment. This can be attributed to the diffusion phenomena that took place. As mentioned above, iron atoms diffuse into the copper coating. The copper coating contains 0.3–1.5% Fe, so the solubility of iron in copper is exceeded (Fig. 14). Precipitation of an Fe phase from the Cu phase may be suppressed by the high cooling rates. Also, copper is strengthened by the presence of nickel atoms. The copper–nickel system displays complete solid solubility (Hume Rothery's rules, which control the tendencies for the formation of substitutional solid solutions, are fully satisfied) and copper and nickel atoms are randomly located at the lattice points of a face centred cubic lattice. The introduction of solute atoms (nickel and iron) into solid solution in the solvent–atom lattice (copper) produces an alloy that is stronger than the pure metal (copper) [15]. The strengthening was not very intensive because the

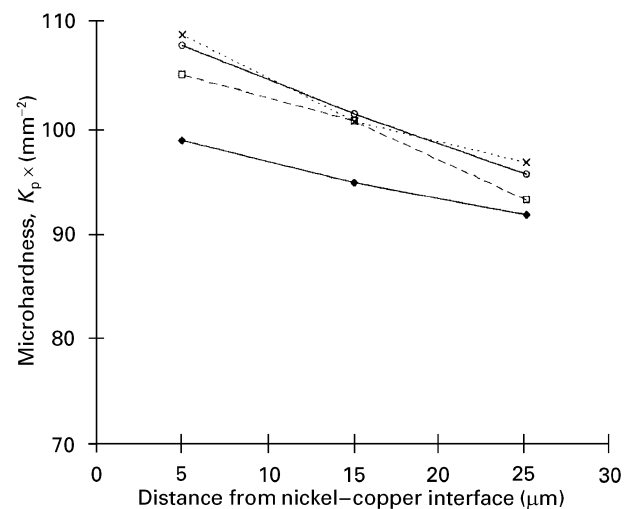


Figure 12 Microhardness of copper as a function of distance from the nickel–copper interface for different values of laser power densities (thickness of copper coating, 30  $\mu\text{m}$ ; 20 pulses per step): ( $\blacklozenge$ ) before laser treatment; ( $\times$ ) 200  $\text{MW cm}^{-2}$ ; ( $\circ$ ) 300  $\text{MW cm}^{-2}$ ; ( $\square$ ) 350  $\text{MW cm}^{-2}$ .

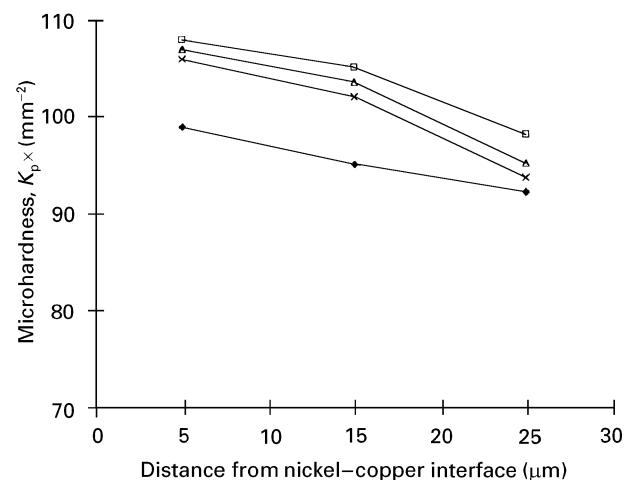


Figure 13 Microhardness of copper as a function of distance from the nickel–copper interface for different numbers of pulses per step (thickness of copper coating, 30  $\mu\text{m}$ ; 300  $\text{MW cm}^{-2}$  power density): ( $\blacklozenge$ ) before laser treatment, ( $\square$ ) 10 p.p.s., ( $\triangle$ ) 50 p.p.s., ( $\times$ ) 250 p.p.s.

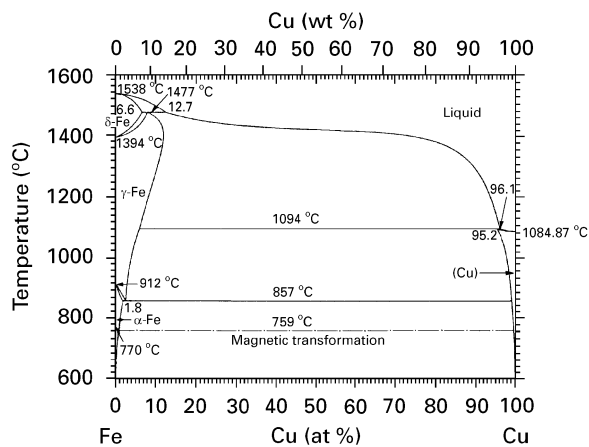


Figure 14 Fe–Cu equilibrium phase diagram [14].

concentrations of nickel and iron atoms in the copper coating were very small.

#### 4. Conclusions

Surface treatment of copper-coated mild steel with a high intensity excimer laser was carried out: the main conclusions of this study are given below.

1. Laser-induced surface structures are dependent upon the density of the laser power.

2. The roughness of the surface is found to be dependent on the number of pulses.

3. Iron atoms are found to diffuse into the copper coating through the nickel strike. Nickel atoms are found to diffuse into the copper coating. Diffusion of copper atoms into the thin nickel coating is also observed.

4. A slight increase of copper microhardness is observed due to solid solution strengthening of copper by iron and nickel atoms.

#### Acknowledgements

The authors wish to thank Dr J. Inglese (Hellenic Force) for performing the EDX analyses of laser-treated specimens.

#### References

1. F. OLSEN, C. BAGGER, T. KRISTENSEN, H. JORGENSEN and O. GREGERSEN, "Laser materials processing", 3rd edn (Technical University of Denmark, 1992) pp. 3.5, 3.10, 3.11, 7.9.
2. W. K. WANG and F. SPAEPEN, *J. Appl. Phys.* **58** (1985) 4477.
3. C.-J. LIN and F. SPAEPEN, *Acta Metall.* **34** (1986) 1367.
4. J.-P. HIRVONEN, J. W. MAYER, M. NASTASI and D. STONE, *Nucl. Instrum. Methods B* **23** (1987) 487.
5. T. R. JERVIS, M. NASTASI, T. G. ZOCCO and J. A. MARTIN, *Appl. Phys. Lett.* **53** (1988) p. 75.
6. A. MICHAELIDIS and C. N. PANAGOPOULOS, in Proceedings of the Ninth Greek Conference on Lasers, edited by the Greek Electro-optical Society, Athens, 1992, p. 250.
7. C. N. PANAGOPOULOS, G. CHRISTOU and G. DAURELIO, *Trans. Inst. Metal Finish.* **71** (1993) 65.
8. D. K. DAS, *Surface Coating Technol.* **64** (1994) 11.
9. M. TAYAL and K. MUKHERJEE, *J. Mater. Sci.* **29** (1994) 5699.
10. L. M. WEISENBERG, "Surface Cleaning, Finishing and Coating", Vol. 5, 9th Edn (American Society for Metals, Metals Park, OH, 1983).
11. J. T. LUXON and D. E. PARKER, "Industrial lasers and their applications", 2nd Edn (Prentice-Hall, Englewood Cliffs, NJ, 1992) pp. 251–5.
12. W. M. STEEN, "Laser material processing" (Springer-Verlag, London, 1991) pp. 47–50.
13. T. R. ANTHONY and H. E. CLINE, *J. Appl. Phys.* **48** (1977) 3888.
14. B. MASSALSKI, "Binary alloy phase diagrams", Vol. 1 (American Society for Metals, Metals Park, OH, 1986).
15. G. E. DIETER, "Mechanical metallurgy" (McGraw-Hill, London, 1988) pp. 203–7.

Received 6 February  
and accepted 17 July 1996